

High mobility and high on/off ratio field-effect transistors based on chemical vapor deposited single-crystal MoS₂ grains

Wei Wu^{1,2}, Debtanu De^{3,4}, Su-Chi Chang^{2,5}, Yanan Wang¹, Haibing Peng^{3,4},
Jiming Bao¹ and Shin-Shem Pei^{1,2,a)}

¹ Department of Electrical and Computer Engineering, University of Houston, Houston, TX 77204, USA

² Center for Advanced Materials, University of Houston, Houston, TX 77204, USA

³ Department of Physics, University of Houston, Houston, TX 77204, USA

⁴ Texas Center for Superconductivity, University of Houston, Houston, TX 77204, USA

⁵ Materials Engineering Program, University of Houston, Houston, TX 77204, USA

We report field-effect transistors (FETs) with single-crystal molybdenum disulfide (MoS₂) channels synthesized by chemical vapor deposition (CVD). For a bilayer MoS₂ FET, the mobility is $\sim 17 \text{ cm}^2\text{V}^{-1}\text{s}^{-1}$ and the on/off current ratio is $\sim 10^8$, which are much higher than those of FETs based on CVD polycrystalline MoS₂ films. By avoiding the detrimental effects of the grain boundaries and the contamination introduced by the transfer process, the quality of the CVD MoS₂ atomic layers deposited directly on SiO₂ is comparable to the best exfoliated MoS₂ flakes. It shows that CVD is a viable method to synthesize high quality MoS₂ atomic layers.

^{a)} Author to whom correspondence should be addressed. Electronic mail: spei@uh.edu

The single-layer (SL) graphene has a linear Dirac-like band structure with no bandgap, which leads to the formation of massless Dirac fermions with remarkable electronic properties, e.g., an effective speed of light $v_F \approx 10^6 \text{ ms}^{-1}$ and a room temperature mobility of $200,000 \text{ cm}^2\text{V}^{-1}\text{s}^{-1}$. However, the lack of a bandgap also limits the application of graphene. Recently, transition metal dichalcogenides (TMDs), molybdenum disulfide (MoS_2) in particular, have attracted a lot of attention. The bulk MoS_2 is a semiconductor with an indirect bandgap of $\sim 1.3 \text{ eV}$ and the SL MoS_2 has a direct bandgap $\sim 1.8 \text{ eV}$.^{1,2,3} Therefore, MoS_2 could complement graphene for many electronic and photonic applications. However, studies of mechanically exfoliated MoS_2 on SiO_2 found the room temperature mobility is $< 10 \text{ cm}^2\text{V}^{-1}\text{s}^{-1}$ for SL- MoS_2 and $10\sim 15 \text{ cm}^2\text{V}^{-1}\text{s}^{-1}$ for bilayer MoS_2 ,^{4,5} which are substantially lower than the measured $\sim 200 \text{ cm}^2\text{V}^{-1}\text{s}^{-1}$ of the bulk MoS_2 ,⁶ or the calculated $\sim 410 \text{ cm}^2\text{V}^{-1}\text{s}^{-1}$ of intrinsic n-type SL- MoS_2 , which is limited only by optical phonon scattering.⁷ The lower than expected mobility is partially due to the long ranged charge disorder or short ranged disorder caused by chemical bonding or roughness at the interfaces.⁸ Furthermore, the mechanical exfoliation process cannot be scaled up for practical applications.

Only recently, large-area of SL and few-layer MoS_2 films have been synthesized by chemical vapor deposition (CVD),^{9,10} sulfurization of MoO_3 ,¹¹ or thermolysis of $(\text{NH}_4)\text{MoS}_4$.¹² CVD has been demonstrated as the most practical method of synthesizing large-area and high quality graphene,¹³ boron nitride¹⁴ and BCN nanosheets.¹⁵ However, devices fabricated from these polycrystalline MoS_2 films are still substantially inferior to their exfoliated counterparts.^{4,16} One possible cause of the degradation of performance is the detrimental effects of the grain boundaries, which can be avoided in the case of graphene by going to a seeded growth single-

crystal array approach by CVD to place graphene grains at predetermined locations where devices will be located.¹⁷

In this paper, we report the construction of field-effect transistors (FETs) based on single-crystal bilayer and few-layer MoS₂ grains. SL, bilayer and few-layer grains with sizes up to 20 μm were synthesized directly on SiO₂ by CVD. Bilayer and few-layer FETs offer higher on-state current than the SL-MoS₂ FET, while maintain high on/off current ratios.⁵ With a single-crystal bilayer MoS₂ conducting channel, we have achieved a superior mobility of 17.3 cm²V⁻¹s⁻¹ and a current on/off ratio of 4x10⁸ in a back-gated MoS₂ FET.

Our CVD-growth method of single-crystal MoS₂ grains is a modification of what is described in Ref. ¹⁰ for continuous MoS₂ films. However, we do not use seeds as nucleation centers to initiate the growth. Single-crystal MoS₂ grains were synthesized in a conventional horizontal quartz tube furnace with sulfur and MoO₃ powders as source materials. The MoO₃ (0.1 g, Alfa, 99.5%) was placed in an alumina boat and loaded into the center uniform-temperature zone of the furnace. However, we found the residues deposited on the wall of the quartz tube furnace also contribute to the subsequent MoS₂ growth, which is not the focus of this paper and will be discussed in detail in another paper.

A piece of Si wafer with 300 nm SiO₂ layer was put downstream in a separate boat as substrate. Another alumina boat with 0.4 g sulfur (Alfa, 99.5%) was placed upstream in a low-temperature zone. Before growth, the furnace was evacuated down to ~70 mTorr and back-filled with Ar gas to ambient pressure. In the flow atmosphere of 100 sccm Ar, the furnace was heated to 700 °C at the center zone in 60 min subsequently up to 1100 °C in 130 min. The temperature

of the sulfur and the substrate was increased concurrently to ~ 100 °C and ~ 700 °C, respectively. After 20 min, the furnace was cooled down naturally to room temperature.

Raman spectroscopy is used as a non-destructive method to characterize crystalline quality and thickness of MoS₂ grains. Representative Raman spectra of SL and bilayer MoS₂ grains are shown in Fig. 1. For MoS₂ crystals, two characteristic Raman active modes, E_{2g}¹ and A_{1g}, are found. They are associated with the in-plane and out-of-plane vibration of sulfides, respectively.¹⁸ It has been reported that the peak frequency difference between E_{2g}¹ and A_{1g} (Δ) can be used to identify the number of MoS₂ layers.^{9,11,19} Figures 2(a) and 2(b) show Raman intensity mappings of E_{2g}¹ at 383 cm⁻¹ and A_{1g} at 405 cm⁻¹ of a triangular shape MoS₂ grain, which confirms the thickness and quality uniformity of the CVD grains. A Δ of 22 cm⁻¹ suggests the grain is a bilayer MoS₂ crystal. For SL MoS₂, $\Delta = 18$ cm⁻¹ in our system. In Fig. 3, a typical photoluminescence (PL) spectrum of the bilayer grain presents two emission peaks at 676 nm and 630 nm, known as A1 and B1 direct excitonic transitions, respectively.²⁰ The PL result is also consistent with recent studies of large-area CVD MoS₂ films.^{10,11}

The Individual MoS₂ grains were first visually inspected and selected under an optical microscope and their positions were recorded with respect to predefined marks. The numbers of MoS₂ layers of individual grains were determined by Raman spectroscopy. Subsequently, MoS₂ grains were fabricated into back-gated FETs with the standard microelectronics processes following steps similar to those described in Ref. 21. The patterned drain and source metal contact electrodes of 45 nm Pd (on top of a 5 nm adhesion layer of Cr) were fabricated on the selected MoS₂ grains by electron-beam lithography and a lift-off process.

Figure 4(a) shows an optical microscopy image of the FET under study in Figs. 4(b)-(d). The channel of the FET is bilayer MoS₂ determined by Raman spectroscopy. The degenerately

doped Si substrate, which is separated from the MoS₂ channel by a 300 nm SiO₂, is used as a back gate to tune the charge carrier density in the MoS₂ channel via the application of a back gate voltage V_G. Room temperature electrical measurements were performed under vacuum (10⁻⁵–10⁻⁶ Torr) in a Lakeshore TTP6 cryogenic probe station.

Figure 4(b) shows the drain current I_{DS} at fixed drain–source voltage, V_{DS}=+500mV, as a function of the applied back-gate voltage V_G, for the device shown in Fig. 4(a). The device is an n-channel normally-on FET. The field-effect mobility is determined using the formula: $\mu = (L/WC_{ox})\Delta G/\Delta V_G$,²² where $G = I_{DS}/V_{DS}$ is the conductance and $\Delta G/\Delta V_G = (1/V_{DS})(\Delta I_{DS}/\Delta V_G)$ is determined from the slope of a linear-fit of the data with the back-gate voltage ranges from V_G=+80V to V_G=+100V. L = 1 μm is the length and W = 3.6 μm is the width of the MoS₂ channel determined from Fig. 2(a). C_{ox} = ε₀ε_r/d is the capacitance per unit area, where d = 300 nm is the thickness of the SiO₂ layer with ε₀ = 8.854x10⁻¹² Fm⁻¹ being the free-space permittivity and ε_r = 3.9 being the relative permittivity of SiO₂. The field-effect mobility of the CVD bilayer MoS₂ is determined to be 17.3 cm²V⁻¹s⁻¹ comparing to the previously reported 0.02 cm²V⁻¹s⁻¹ of CVD SL-MoS₂,¹⁰ and 0.04 cm²V⁻¹s⁻¹ of the CVD few-layer MoS₂.⁹ The much higher mobility of our device may be partially due to the elimination of grain boundary scattering as we reported previously for the CVD graphene.¹⁷ Actually, the 17.3 cm²V⁻¹s⁻¹ mobility of the CVD bilayer MoS₂ grain is comparable to the 0.1-10 cm²V⁻¹s⁻¹ reported for exfoliated SL-MoS₂,⁴ and the 10-15 cm²V⁻¹s⁻¹ for exfoliated bilayer MoS₂.⁵ Another order of magnitude improvement is expected if a high-κ dielectric is applied on the top of the MoS₂ channel to reduce the Coulomb effect.^{4,5,23}

In Fig. 4(c), the drain current I_{DS} is re-plotted on a logarithmic scale as a function of V_G. At V_G = -100 V, the MoS₂ channel of the FET is pinched off with an off-state I_{DS} < 0.1 pA. The

on-state I_{DS} is $> 30 \mu\text{A}$ with $V_G = +100 \text{ V}$. The corresponding on/off current ratio is 4×10^8 , which is higher than the $\sim 10^4$ on/off current ratio reported for CVD polycrystalline MoS_2 films,¹⁰ and comparable to the $\sim 10^8$ of the exfoliated SL- MoS_2 flakes.⁴

Figure 4(d) shows the room temperature transfer characteristics of the FET, i.e. the dependence of drain current on the back-gate voltage at various drain-source voltages. Due to the thick SiO_2 back-gate dielectric, no drain current saturation is observed. For comparison, another back-gated FET with a few-layer (< 5 layers) MoS_2 channel was also fabricated, the mobility is also $\sim 17 \text{ cm}^2\text{V}^{-1}\text{s}^{-1}$, while the on/off current ratio might be slightly lower, but still $> 10^4$. Most recently, ven der Zande et al. also reported the electrical characteristics of CVD single-crystal MoS_2 grains. The mobility measured within a grain was reported to be $3\text{-}4 \text{ cm}^2\text{V}^{-1}\text{s}^{-1}$ and the on/off current ratio was in the range of 10^5 to 10^7 .²⁴ Our results are consistent with their findings.

It is well known that the best reported mobility of graphene on SiO_2 is limited to $10,000 \text{ cm}^2\text{V}^{-1}\text{s}^{-1}$ primarily due to the Coulomb effect.²⁵ For exfoliated multilayer MoS_2 on SiO_2 , the room temperature mobility can be substantially enhanced by engineering the dielectric environment. For example, multilayer MoS_2 has exhibited a mobility $> 100 \text{ cm}^2\text{V}^{-1}\text{s}^{-1}$ when sits on a 50-nm thick atomic layer deposited (ALD) Al_2O_3 ,¹⁶ and $470 \text{ cm}^2\text{V}^{-1}\text{s}^{-1}$ on 50-nm thick spin-coated PMMA.⁸ Further enhancement of the MoS_2 mobility can be achieved by applying appropriate gate dielectric on the top of MoS_2 channel. A mobility as high as $\sim 200 \text{ cm}^2\text{V}^{-1}\text{s}^{-1}$ was achieved with a $\text{HfO}_2/\text{SL-MoS}_2/\text{SiO}_2$ structure, which also exhibits a high on/off ratio ($\sim 10^8$) and low subthreshold swing ($\sim 70 \text{ mV}$ per decade).⁴ Thus, in addition to fundamental scientific interests, MoS_2 FETs could be an attractive candidate for low power electronics, e.g. thin-film

transistors (TFTs) in the next generation high-resolution liquid crystal (LCD) or organic light-emitting diode (OLED) displays.²⁶

In conclusion, we report the electrical characteristics of back gated FETs fabricated on single-crystal MoS₂ grains synthesized by CVD on SiO₂. A FET with a bilayer MoS₂ channel has a mobility $\sim 17 \text{ cm}^2\text{V}^{-1}\text{s}^{-1}$ and an on/off current ratio $\sim 10^8$, while the FET with a few-layer MoS₂ channel exhibits comparable mobility, but slightly lower on/off current ratio. Another order of magnitude improvement of mobility is expected by dielectric engineering to reduce the Coulomb effect. The results suggest that CVD is a viable method to synthesize high quality MoS₂ grains with performance comparable to the best mechanically exfoliated MoS₂ flakes, and MoS₂ FETs are promising candidates for low power electronics.

REFERENCES

- ¹ G. L. Frey, S. Elani, M. Homyonfer, Y. Feldman, and R. Tenne, *Phys Rev B* **57** (11), 6666 (1998).
- ² K. F. Mak, C. Lee, J. Hone, J. Shan, and T. F. Heinz, *Phys Rev Lett* **105** (13) (2010).
- ³ T. Cao, G. Wang, W. P. Han, H. Q. Ye, C. R. Zhu, J. R. Shi, Q. Niu, P. H. Tan, E. Wang, B. L. Liu, and J. Feng, *Nat Commun* **3** (2012).
- ⁴ B. Radisavljevic, A. Radenovic, J. Brivio, V. Giacometti, and A. Kis, *Nat Nanotechnol* **6** (3), 147 (2011).
- ⁵ H. Wang, L. L. Yu, Y. H. Lee, Y. M. Shi, A. Hsu, M. L. Chin, L. J. Li, M. Dubey, J. Kong, and T. Palacios, *Nano Lett* **12** (9), 4674 (2012).
- ⁶ R. Fivaz and E. Mooser, *Phys Rev* **163** (3), 743 (1967).
- ⁷ K. Kaasbjerg, K. S. Thygesen, and K. W. Jacobsen, *Phys Rev B* **85** (11) (2012).
- ⁸ Wenzhong Bao, Xinghan Cai, Dohun Kim, Karthik Sridhara, and Michael S. Fuhrer, *Applied Physics Letters* **102** (2013).
- ⁹ Y. J. Zhan, Z. Liu, S. Najmaei, P. M. Ajayan, and J. Lou, *Small* **8** (7), 966 (2012).
- ¹⁰ Y. H. Lee, X. Q. Zhang, W. J. Zhang, M. T. Chang, C. T. Lin, K. D. Chang, Y. C. Yu, J. T. W. Wang, C. S. Chang, L. J. Li, and T. W. Lin, *Adv Mater* **24** (17), 2320 (2012).
- ¹¹ Y. C. Lin, W. J. Zhang, J. K. Huang, K. K. Liu, Y. H. Lee, C. T. Liang, C. W. Chu, and L. J. Li, *Nanoscale* **4** (20), 6637 (2012).
- ¹² K. K. Liu, W. J. Zhang, Y. H. Lee, Y. C. Lin, M. T. Chang, C. Su, C. S. Chang, H. Li, Y. M. Shi, H. Zhang, C. S. Lai, and L. J. Li, *Nano Lett* **12** (3), 1538 (2012).
- ¹³ Qingkai Yu, Jie Lian, Sujitra Siriponglert, Hao Li, Yong P. Chen, and Shin-Shem Pei, *Applied Physics Letters* **93** (11) (2008); Alfonso Reina, Xiaoting Jia, John Ho, Daniel Nezich, Hyungbin Son, Vladimir Bulovic, Mildred S. Dresselhaus, and Jing Kong, *Nano Lett* **9** (1), 30 (2009);
K. S. Kim, Y. Zhao, H. Jang, S. Y. Lee, J. M. Kim, J. H. Ahn, P. Kim, J. Y. Choi, and B. H. Hong, *Nature* **457** (7230), 706 (2009); Xuesong Li, Weiwei Cai, Jinho An, Seyoung Kim, Junghyo Nah, Dongxing Yang, Richard Piner, Aruna Velamakanni, Inhwa Jung, Emanuel Tutuc, Sanjay K. Banerjee, Luigi Colombo, and Rodney S. Ruoff, *Science* **324** (5932), 1312 (2009).
- ¹⁴ L. Song, L. J. Ci, H. Lu, P. B. Sorokin, C. H. Jin, J. Ni, A. G. Kvashnin, D. G. Kvashnin, J. Lou, B. I. Yakobson, and P. M. Ajayan, *Nano Lett* **10** (8), 3209 (2010).

- 15 L. Ci, L. Song, C. H. Jin, D. Jariwala, D. X. Wu, Y. J. Li, A. Srivastava, Z. F. Wang, K. Storr, L.
Balicas, F. Liu, and P. M. Ajayan, *Nat Mater* **9** (5), 430 (2010).
- 16 S. Kim, A. Konar, W. S. Hwang, J. H. Lee, J. Lee, J. Yang, C. Jung, H. Kim, J. B. Yoo, J. Y.
Choi, Y. W. Jin, S. Y. Lee, D. Jena, W. Choi, and K. Kim, *Nat Commun* **3** (2012).
- 17 Q. Yu, L. A. Jauregui, W. Wu, R. Colby, J. Tian, Z. Su, H. Cao, Z. Liu, D. Pandey, D. Wei, T. F.
Chung, P. Peng, N. P. Guisinger, E. A. Stach, J. Bao, S. S. Pei, and Y. P. Chen, *Nat Mater* **10** (6),
443 (2011); Wei Wu, Luis A. Jauregui, Zhihua Su, Zhihong Liu, Jiming Bao, Yong P. Chen,
and Qingkai Yu, *Adv Mater* **23** (42), 4898 (2011).
- 18 T. J. Wieting and J. L. Verble, *Phys Rev B* **3** (12), 4286 (1971); S. J. Sandoval, D. Yang, R. F.
Frindt, and J. C. Irwin, *Phys Rev B* **44** (8), 3955 (1991).
- 19 C. Lee, H. Yan, L. E. Brus, T. F. Heinz, J. Hone, and S. Ryu, *Acs Nano* **4** (5), 2695 (2010).
- 20 A. Splendiani, L. Sun, Y. B. Zhang, T. S. Li, J. Kim, C. Y. Chim, G. Galli, and F. Wang, *Nano*
Lett **10** (4), 1271 (2010).
- 21 D. De, J. Manongdo, S. See, V. Zhang, A. Guloy, and H. B. Peng, *Nanotechnology* **24** (2)
(2013).
- 22 A. Ayari, E. Cobas, O. Ogundadegbe, and M. S. Fuhrer, *J Appl Phys* **101** (1) (2007).
- 23 H. Qiu, L. J. Pan, Z. N. Yao, J. J. Li, Y. Shi, and X. R. Wang, *Applied Physics Letters* **100** (12)
(2012); H. Liu and P. D. D. Ye, *Ieee Electr Device L* **33** (4), 546 (2012).
- 24 Arend M. van der Zande, Pinshane Y. Huang, Daniel A. Chenet, Timothy C. Berkelbach,
Youmeng You, Gwan-Hyoung Le, Tony F. Hein, David R. Reichman, David A. Mulle, and
James C. Hone, *arXiv:1301.1985* (2013).
- 25 W. J. Zhu, V. Perebeinos, M. Freitag, and P. Avouris, *Phys Rev B* **80** (23) (2009).
- 26 T. Kamiya, K. Nomura, and H. Hosono, *Sci Technol Adv Mat* **11** (4) (2010).

FIGURES

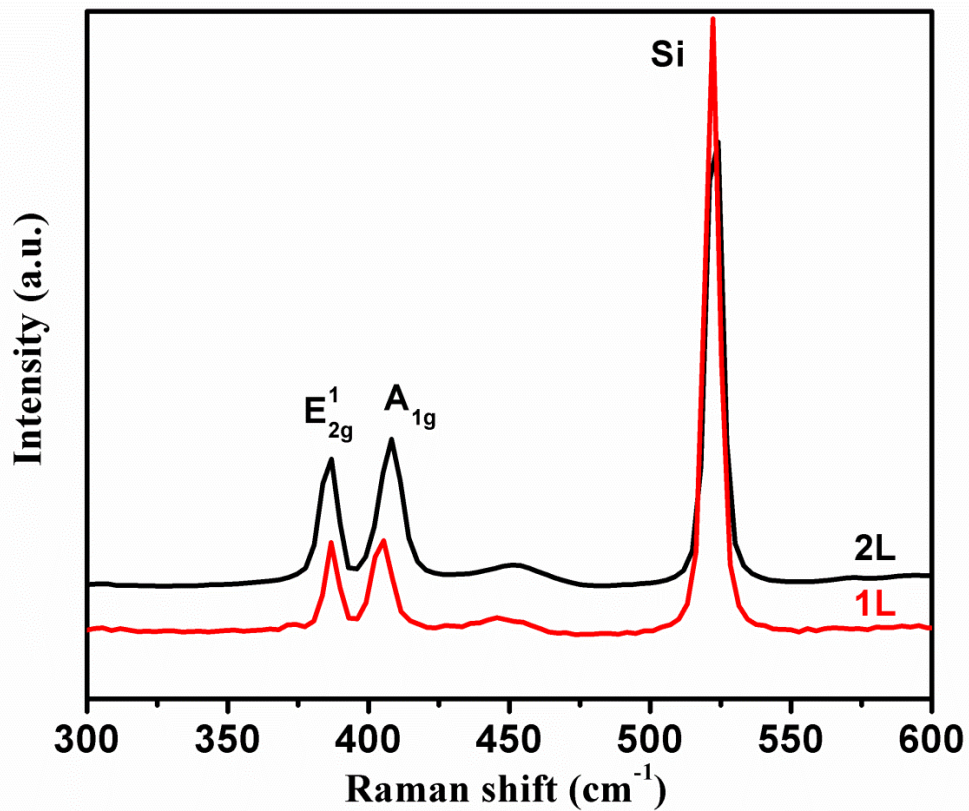


FIG 1. Raman spectra of typical single-layer and bilayer MoS₂ crystals. E_{2g}¹ at 383 cm⁻¹ and A_{1g} at 405 cm⁻¹ for bilayer; E_{2g}¹ at 384 cm⁻¹ and A_{1g} at 402 cm⁻¹ for single layer. The laser excitation wavelength is 532 nm.

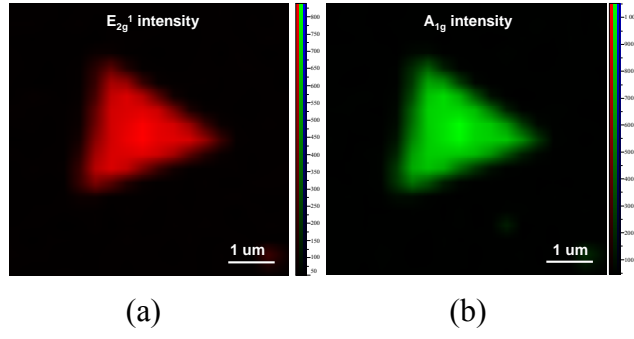


FIG. 2. Raman intensity mappings of (a) E_{2g}^1 and (b) A_{1g} of a typical bilayer MoS_2 grain.

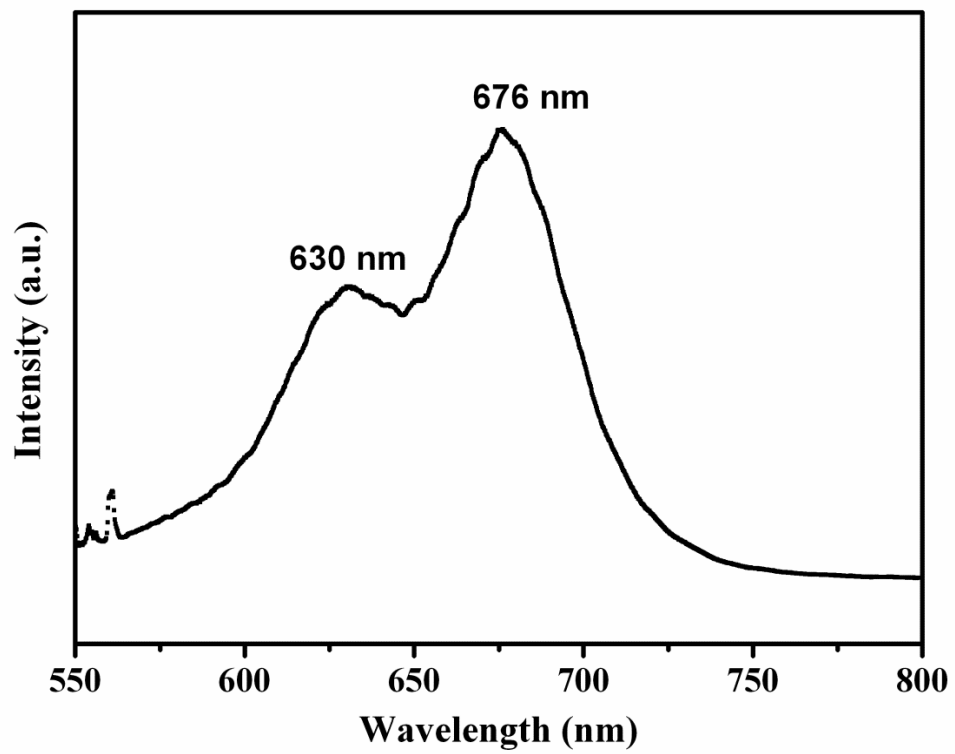


FIG. 3. Photoluminescence spectrum of a typical bilayer MoS₂ crystal. The laser excitation wavelength is 532 nm.

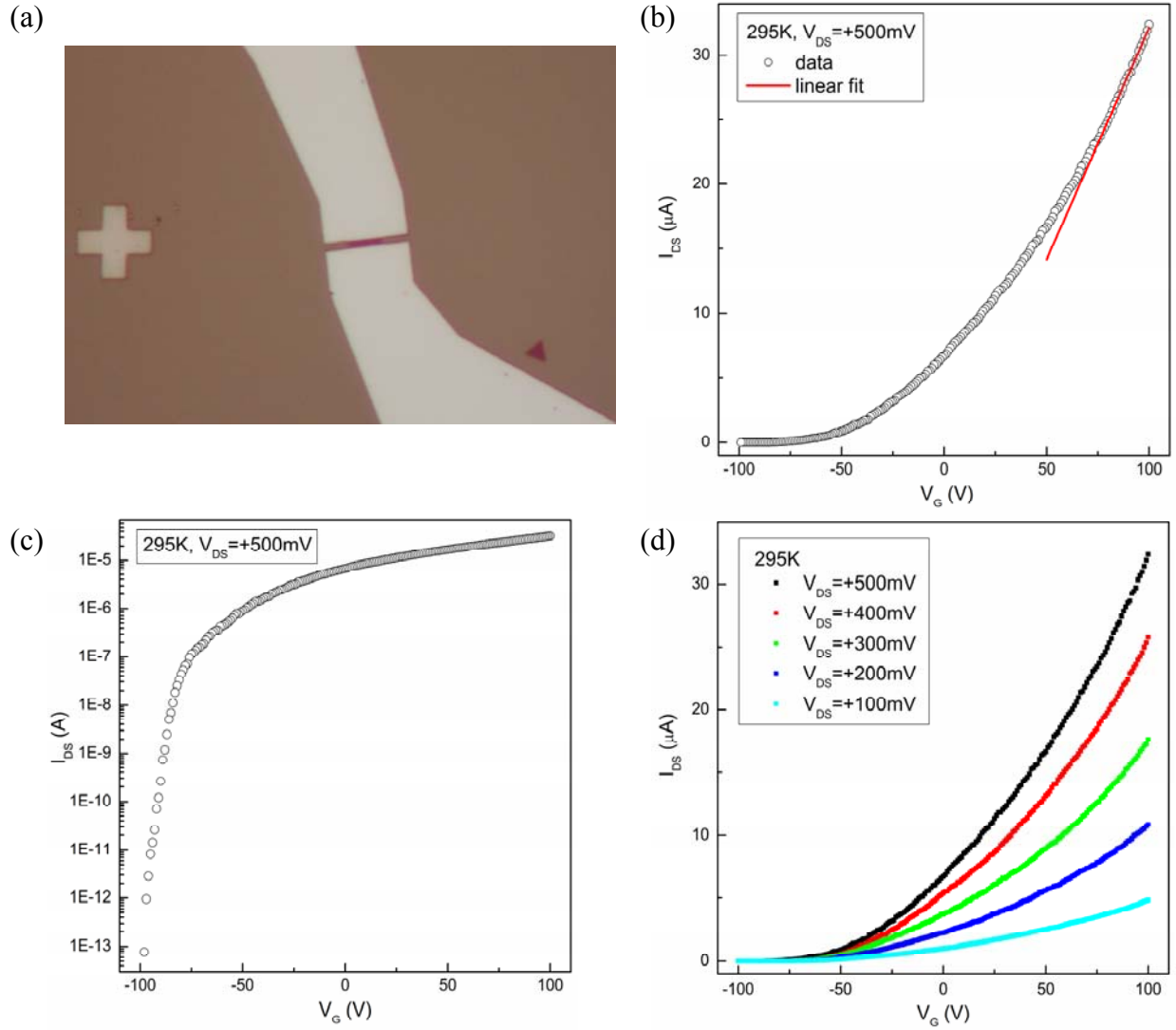


FIG. 4. (a) Optical image of the device. The gap between the two electrodes acrossing the MoS₂ grain is 1 μ m. (b) (Open circles) Drain-source current I_{DS} as a function of back-gate voltage V_G at fixed drain-source bias voltage $V_{DS}=+500$ mV. (Red line) Linear-fit of the data within the back-gate voltage range from $V_G=+80$ V to $V_G=+100$ V. From the linear fit data, the carrier mobility is calculated to be $\mu=17.3$ cm²V⁻¹s⁻¹. (c) Drain-source current I_{DS} plotted in logarithmic scale as a function of back-gate voltage V_G at fixed drain-source bias voltage $V_{DS}=+500$ mV. The optimized current pre-amplifier gain used in the measurement: 100pA/V for $V_G=-100$ V to -90V, 10nA/V for $V_G=-89$ V to -80V, 500nA/V for $V_G=-79$ V to -40V and 10 μ A/V for $V_G=-40$ V to +100V. (d) Drain-source current I_{DS} as a function of back-gate voltage V_G at drain-source bias voltages $V_{DS}=+500$ mV, $=+400$ mV, $=+300$ mV, $=+200$ mV and $=+100$ mV.